HHS Public Access

Author manuscript

Int J Cancer. Author manuscript; available in PMC 2016 March 01.

Published in final edited form as:

Int J Cancer. 2015 March 1; 136(5): E242–E251. doi:10.1002/ijc.29198.

Divergence(s) in Nodal Signaling Between Aggressive Melanoma and Embryonic Stem Cells

Zhila Khalkhali-Ellis[*,†], **Dawn A. Kirschmann**[*,†,¥], **Elisabeth A. Seftor**[*,†], **Alina Gilgur**[*], **Thomas M. Bodenstine**[*], **Andrew P. Hinck**[‡], and **Mary J.C. Hendrix**[*,†]

[*]Cancer Biology and Epigenomics Program, Stanley Manne Children's Research Institute, Ann & Robert H. Lurie Children's Hospital of Chicago, 225 E. Chicago Ave, Box 222, Chicago, IL, 60611

[†]Robert H. Lurie Comprehensive Cancer Center, Northwestern University Feinberg School of Medicine, 303 E. Superior Street, Chicago, IL 60611

[‡]Department of Biochemistry, University of Texas Health Sciences Center, San Antonio, TX 78229

Abstract

The significant role of the embryonic morphogen Nodal in maintaining the pluripotency of embryonic stem cells is well documented. Interestingly, the recent discovery of Nodal's re-expression in several aggressive and metastatic cancers has highlighted its critical role in self renewal and maintenance of the stem cell-like characteristics of tumor cells, such as melanoma. However, the key TGFβ/Nodal signaling component(s) governing Nodal's effects in metastatic melanoma remain mostly unknown. By employing receptor profiling at the mRNA and protein level(s), we made the novel discovery that embryonic stem cells and metastatic melanoma cells share a similar repertoire of Type I serine/threonine kinase receptors, but diverge in their Type II receptor expression. Ligand:receptor crosslinking and native gel binding assays indicate that metastatic melanoma cells employ the heterodimeric TGFβ receptor I/TGFβ receptor II (TGFβRI/TGFβRII) for signal transduction, whereas embryonic stem cells use the Activin receptors I and II (ACTRI/ACTRII). This unexpected receptor usage by tumor cells was tested by: neutralizing antibody to block its function; and transfecting the dominant negative receptor to compete with the endogenous receptor for ligand binding. Furthermore, a direct biological role for TGFβRII was found to underlie vasculogenic mimicry (VM), an endothelial phenotype contributing to vascular perfusion and associated with the functional plasticity of aggressive melanoma. Collectively, these findings reveal the divergence in Nodal signaling between embryonic stem cells and metastatic melanoma that can impact new therapeutic strategies targeting the re-emergence of embryonic pathways.

Keywords

Nodal; Melanoma; TGF-β RII; TGF-β RI; Embryonic Stem Cells

Correspondence: Zhila Khalkhali-Ellis, Ph.D. Stanley Manne Children's Research Institute 225 E Chicago Ave, Box 222 Chicago, IL 60611 T:773-755-6353 F:773-755-6594 zellis@luriechildrens.org.

[¥]Present address: HLA & Molecular Diagnostics Laboratory Department of Pathology and Laboratory Medicine Ann and Robert H. Lurie Children's Hospital of Chicago 225 E. Chicago Ave, Box 82 Chicago, IL 60611

INTRODUCTION

It is becoming evident that metastatic tumor cells share similar signaling pathways with embryonic stem cells to sustain plasticity and growth; however, major regulators of these pathways are often missing in tumor cells, thus allowing uncontrolled tumorigenicity to occur. A noteworthy example is Nodal, a member of the TGFβ superfamily and a critical embryonic morphogen and regulator of cell fate (1,2). Nodal is quintessential in maintaining the pluripotency of human embryonic stem cells (hESCs, 3,4) and is exquisitely regulated by a major inhibitors Lefty A,B (3,5). The recent discovery of the re-emergence of Nodal signaling in several aggressive cancers (6-11), accompanied by the epigenetic silencing of Lefty (12), has promoted Nodal as a promising new therapeutic target, and signifies the importance of achieving a better understanding of the mechanism(s) enabling Nodal signaling in tumor cells. Seminal studies in embryonic stem cell biology have established that similar to other members of the TGFβ superfamily, Nodal exerts its downstream effects by binding the heterodimeric complex composed of type I (ALK4/7) and type II (Activin receptor IIB, ACTRIIB) serine/threonine kinase receptors, which leads to phosphorylation of ALK4/7 by ACTRIIB (1,2,13-15). Receptor engagement phosphorylates Smads2/3 and regulates Nodal target genes via association with Smad4. However, the signaling pathway(s) utilized by melanoma cells to propagate Nodal's effect remain(s) mostly anecdotal and unexplored.

By employing hESCs as the standard canonical pathway control, we have performed receptor profiling both at the mRNA and protein levels, to determine the commonality (or divergence) in Nodal's signaling machinery in metastatic melanoma cells compared with human embryonic stem cells. Our studies reveal distinct differences in the expression of ACTRII and Cripto (TDGF1), the GPI-linked protein and co-receptor involved in TGFβ/Nodal signaling (15-17), between hESCs and aggressive melanoma cells. Specifically, melanoma cells displayed minimal expression of ACTRII and Cripto, but presented with abundant levels of TGFβ receptor II (TGFβRII). This unexpected observation prompted the query of signaling mechanisms utilized by these aggressive tumor cells to support their plasticity related to Nodal's effect. Using vasculogenic mimicry (VM) as a biological measurement of functional plasticity, we discovered a direct role for TGFβRII underlying melanoma VM, which may impact new therapeutic strategies targeting the re-emergence of embryonic signaling pathways in tumor cells.

METHODS

Cell Culture

Well characterized aggressive human cutaneous melanoma cell lines C8161, MV3 (18,19) and non-aggressive UACC1273 (20) were cultured in RPMI 1640 supplemented with 10% fetal calf serum (FCS). The non-aggressive c81-61 cell line (21) was maintained in Ham's F-10 medium supplemented with 15% FCS, 1% Mito+ (BD Bioscience) and gentamicine sulfate. Human embryonic stem cells H9 and H14 (Wicell) were cultured on CellStart in StemPro hESC SFM defined media (Life Technologies). Normal human melanocytes were maintained in Medium 254 supplemented with Human Melanocyte Growth Supplement

(Life Technologies). All cell lines were authenticated by short tandom repeat genotyping by PCR amplification at the Molecular Diagnostic/HLA Typing Core at Lurie Children's Hospital of Chicago, and were tested for mycoplasma contamination using PCR-based detection system (Roche).

Real-Time PCR

Total RNA was isolated from cells using the PerfectPure RNA Cell Kit (5Prime) according to manufacturer's specifications. Reverse transcription of the total RNA was performed in a Robocycler gradient 96 thermocycler (Agilant). PCR was performed on a 7500 Real Time PCR System (Life Technologies) using TaqMan® gene expression primer/probe sets (*TGFBRII*: Hs00559661_m1, *TGFBRI [ALK5]:*Hs00610319_m1, *ACTRIIA*: Hs00155658_m1, *ACTRIIB*: Hs0069604_m1, Cripto [TDGF1]:Hs02339499_m1, ACTRIB [ALK4]: Hs0024475_m1 and ACTRIC [ALK7]: Hs00377065_m,1 Life Technologies). Briefly, 5 μl cDNA, 1.25 μl 20X Gene Expression Assay Mix, and 12.5 μl 2X TaqMan® Universal PCR Master Mix in a total of 25 μl were amplified with the following thermocycler protocol: 1 cycle at 50°C for 2 min; 1 cycle at 95°C for 10 min; and 33 cycles at 95°C for 15 seconds; 60°C for 1 min. All data were analyzed with the Sequence Detection Software (version 1.2.3, Life Technologies). The expression of each target gene was normalized to an endogenous control gene, RPLPO large ribosomal protein (4333761F, Life Technologies). Each sample testing was performed in triplicate.

TGFβRII Gene Transfection

pTGFβRII/CEP-Zeo/Hygro plasmid (AddGene, #16622) was propagated with ampicillin selection, and was purified using a MaxiPrep kit (Qiagen). The conformation and purity of the plasmid were established by restriction digest and sequencing analysis. UACC1273 cell line was transfected with pTGFβRII/CEP-Zeo/Hygro using Effectine (Qiagen) and SuperFect (Qiagen) transfection methods. Resistant colonies were selected with hygromycin and subcultured to generate stable clones. Clones were analyzed for *TGFRBII* gene expression by RT-PCR analysis (Applied Biosystems), and protein expression by Western blot analysis.

Subcellular Fractionation and Western Blot Analysis

This was performed as previously described (22). Briefly, semi-confluent cultures of stem cell lines (H9 and H14) or melanoma cell lines (C8161, MV3, c81-61, UACC1273) and normal melanocytes were washed with PBS and scraped in buffer A (10mM HEPES buffer pH 7.9 containing 10mM NaCl,1mM DTT, 10% glycerol, 15mM $MgCl_2$, 0.2mM EDTA, 0.1%NP40, protease and phosphatase inhibitor cocktails) and subjected to three cycles of freeze-thaw and centrifuged at 1000xg for 8 min. The supernatant (post-nuclear cytosolic fraction) was collected, and the protein content of each fraction was determined using BCA reagent (BioRad).

Equal amounts of cellular protein from various experimental treatments were subjected to SDS-PAGE and Western blot analysis using specific antibodies to ACTRIB (ALK4), ACTRIIB (Epitomics), VE-cadherin, Smad3 (BD Pharmingen), TGFβ RII, TGFβ RI (ALK5), Smad 4, Nodal and ACTRII (Santa Cruz Biotechnology), Cripto (TDGF1;

Rockland), Smad2[pT8] (Invitrogen), and Smad2/3 [pSer465/467] (Calbiochem). For Western blot of bands excised from Native gels an anti-TGFβ RI antibody raised against residues 26-125 of the extracellular domain of TGFβ RI was used (H-100, Santa Cruz Biotechnology). The reaction products were visualized using the ECL chemiluminescent kit (GE Healthcare). For consistency and when possible, each blot was probed for several antigens and GAPDH served as control for equal loading.

In Vitro Binding Assay and Native Gel Electrophoresis

Human recombinant extracellular domains of TGFβRI (residues 7-91, EDTGFβRI) and TGFβRII (residues15-130, EDTGFβRII) were generated, purified and characterized in the laboratory of Dr. A. P. Hinck (23). Recombinant Nodal (rNodal; R&D Systems, one molar equivalent) was mixed with two molar equivalents of recombinant EDTGFβRII and EDTGFβRI in HEPES buffer (pH 6.5; 30 min, RT). The reaction products were resolved on a 10% native acrylamide gel (pH 8.8) using receptor(s) and ligand alone as control. TGFβ3 binding to EDTGFβRII/EDTGFβRI served as a positive control. The complex formation was detected by Commassie Blue staining of the gel, and the high molecular mass complexes were excised from the gel and analyzed by SDS-PAGE (4-20% acrylamide) and Western blot analysis.

Biotin Labeling and Crosslinking

Carrier-free rNodal (R&D Systems) was Biotin labelled using EZ-Link Sulfo-NHS-LC-Biotin (Thermo Scientific) and according to the manufactures' instruction. Excess Biotin was removed by dialysis, and the labeled product was tested by Western blot and probed by Strepavidin (Sigma). The confluent cultures of hESCs, MV3 and C8161 melanoma cell lines (>90%) were washed several times with PBS and treated with Biotin-labeled rNodal (500ng/ml PBS) for 60min at 37°C. The soluble crosslinker bis (sulfosuccinimidyl) suberate (BS^3,Thermo Scientific) was dissolved in PBS just prior to use and added to the cultures at a final concentration of 20mM, 30min at 4°C (to reduce internalization of the crosslinker). The reaction was quenched by Tris (100mM, pH 7.5), the cells were harvested, and cytosolic and membrane fractions were prepared using Mem-Per™ Membrane Extraction Kit (Thermo Scientific). The protein content of each fraction was determined using BCA reagent (BioRad).

RESULTS AND DISCUSSION

Our studies reveal that at the mRNA level, *ACTRIB (ALK4*) and *TGFβRI (ALK5)* are the predominant type I receptor in hESCs (H9 and H14), melanoma cells (C8161, MV3, c81-61 and UACC1273) and normal human melanocytes (Fig.1A & B). *ACTRIC (ALK 7*) is expressed at high levels in normal melanocytes, low levels in hESCs, and is barely detected in metastatic melanoma cells (Fig. 1C). Of the type II receptors, *ACTRIIA* and *ACTRIIB* are prevalent in hESCs cells with minimal expression of *TGFβRII*. However, *TGFβRII* is amply detected in melanoma cells along with low levels of *ACTRIIA* and negligible levels of *ACTRIIB* (Fig.1D-F). Melanocytes exhibit high levels of *TGFβRII*, considerable levels of *ACTRIIA* and minimum expression of *ACTRII B* (Fig.1D-F). *Cripto*, (*TDGF1*), the GPI-

linked protein and co-receptor involved in TGF-β/Nodal signaling (16,17), is abundant in hESCs and significantly less in melanoma cells or melanocytes (Fig.1G).

Receptor protein expression profiled by Western blot confirmed the mRNA observations for the majority of receptors (Western blots are depicted underneath each respective PCR histogram; Fig. 1 A-G). Considerable heterogeneity was noted in the apparent molecular mass of TGFβRII, generally indicative of different glycosylated and/or phosphorylated status of the receptor. Also noteworthy, metastatic melanoma cells (C8161 and MV3) express higher levels of TGFβRII compared to non-aggressive melanoma cells (c81-61, UACC1273) (Fig.1F), collectively indicating a possible differential response (or sensitivity) to TGFβ (24). Cripto (TDGF1) was abundantly present in hESCs; this protein is heavily glycosylated with both N- and O-linked glycan structures (16) displaying a range of molecular mass (~18-25kDa, Fig.1G). In melanoma cells, only a minor band (~20kDa) was occasionally detected, possibly depicting a moderately glycosylated counterpart (Fig.1G). Immunofluorescence confocal microscopy analyses confirmed minimal cell surface and intracellular Cripto in melanoma cells compared with its strong presence in hESCs (Fig. 1H). This finding corroborates our earlier observation that less than 5% of aggressive melanoma cells are positive for membrane associated Cripto when analyzed by FACS (25).

Based on the current model of Nodal signaling primarily revealed by developmental biology studies, Nodal binds the serine/threonine kinase receptors I (AlK4/7) and II (ACTRIIA and B) and signals through phosphorylated Smad2/3 (13,14, 26-28). The minimal presence of ACTRII(s) and Cripto, concomitant with the abundance of TGFβRII in metastatic melanoma cells, prompted exploring the possibility of an alternative signaling pathway or receptor usage in tumor cells. The possibility of Nodal signaling via TGFβRII was initially explored by sequence alignment with TGFβ isoforms (Sup.Fig.1). Two of the most essential amino acid residues for binding TGFβs to TGFβRII are Arginine 25 and 94 (29, 30). In Nodal, there is possible conservation of Arg 94 but not Arg 25. Initially, we employed an *in vitro* binding assay with the recombinant soluble extracellular domains of TGFβRI (EDTGFβRI) and TGFβRII (EDTGFβRII) and Nodal. The reaction product(s) were resolved on a 10% native acrylamide gel, and complex formation was detected by Commassie Blue staining of the gel. TGFβ3 complex formation with EDTGFβRI/EDTGFβRII served as the positive control. The corresponding complexes were excised from the gel (arrows, Fig.2A) and subjected to reduced SDS-PAGE (4-20% Acrylamide gel) and Western blot analysis and demonstrated a mixture of EDTGFβRI, EDTGFβRII and Nodal (Nodal complex) (Fig.2B). However, compared to the EDTGFβRI/EDTGFβRII/TGFβ3 complex, only a small proportion of EDTGFβRII was in the complex with Nodal, and minimal TGFβ3 abolished Nodal complex formation completely (Fig.2B). Undoubtedly, further structural analyses are required to verify Nodal/TGFβRII binding, the involvement of Arg [X} (or other amino acids in the Nodal molecule), and to establish the distinct mode(s) of receptor binding. In addition, the contribution of factors that might stabilize the Nodal:TGFβRII complex, such as mutual stabilization of TGFβRI by TGFβRII (described for TGFβ receptor complex formation; 31) and the possible involvement of TGFβRIII (Betaglycan) should be considered (32,33).

At the cellular level, Nodal's receptor usage was assessed using Biotin-labeled rNodal crosslinked to the cell surface of hESCs or aggressive melanoma cells. Membrane fractions were analyzed by SDS-PAGE and Western blot to determine Nodal receptor usage. Strepavidin probing of the blot revealed two distinct bands of ~135 and 155kDa in the melanoma cell lines, compared to ~143 band in H9 hESCs (Fig.2C). The latter bands reacted with anti-TGFβRII (Fig. 2D); 135kDa band also reacted with anti-Nodal (Fig.2E), while the 155kDa band was barely detectable with anti-Nodal (data not shown). These observations further supported the *in vitro* binding data and the presence of only a small proportion of TGFβRII in the complex with Nodal. Downstream effects of Nodal binding to TGFβRII were addressed by neutralizing the cell surface receptor protein, and/or employing the small molecule kinase inhibitor SB431542. This kinase inhibitor acts as a competitive ATP binding site of ALK5 (in addition to ALK4 and ALK7), but has no significant inhibitory effect on any of the ALKs (34). Application of SB431542 and neutralizing anti-TGFβRII resulted in down-regulation of Nodal and reduced phosphorylation of Smad3 (pSmad3 432/435) in C8161 melanoma cells (Fig. 3A). In addition, both treatments affected TGFβRII's protein profile. As discussed earlier, TGFβRII is both glycosylated and phosphorylated, which results in a range of molecular mass (~66-90kDa, Fig.3A) when examined under reduced SDS-PAGE conditions. The proportion of these distinct forms was greatly affected by both SB431542 and neutralizing anti-TGFβRII (Fig.3A). Neutralizing pan-TGFβ antibody had no effect on Nodal, but moderately reduced pSmad3 (Fig. 3A). Treatment of metastatic melanoma cell lines with an antibody to Nodal (which reduces the intracellular Nodal protein levels through a negative feedback loop) resulted in considerable attenuation of the TGFβRII protein (and mRNA) levels (Fig.3A). This indicated that in addition to regulating its own level, Nodal exerts a positive feedback effect on TGFβRII expression.

Further validation of Nodal signaling via TGFβRII came from transfection of metastatic melanoma cells with a dominant negative TGFβRII plasmid (DNTGFβRII, 35) lacking the kinase domain (hereafter referred to as DNC8161 or DNMV3 cells). This approach resulted in altered endogenous Nodal protein levels, reduced Smad2/3 phosphorylation (both at serine 423/425 and threonine 8) and cellular proliferation (reduced PCNA expression), comparable to the effects observed in response to SB431542 (Fig.3B &C). Of significance, Smad2 was constitutively phosphorylated on threonine residue 8 in aggressive melanoma cells and transfection with DNTGFβRII resulted in reduced phosphorylation of this threonine residue (Fig.3C). In addition, DNTGFβRII competed with the wild type receptor for ligand binding in metastatic melanoma cells (Fig. 3D).

Nodal's signaling via TGFβRII/TGFβRI in melanoma cells, although unexpected, is not unprecedented. Specifically, the number of known ligands in the TGFβ superfamily (~30) far transcends the limited number of type I (seven) and type II (five) receptors encoded by the human genome (36,37). The combination(s) of type I and II receptors appear(s) to be tissue specific, dictated by physiological conditions, and many ligands in this family converge at the receptor level (1, 2, 25, 38). Notably, in human pulmonary arterial endothelial cells, Bone Morphogenic Protein-9 (BMP-9) can bind BMP-receptor II and ACTRII leading to differential gene expression (39). In addition, functional redundancies

are reported for these two receptors in BMP-2-induced osteoblast differentiation (40). Furthermore, in animal caps of *Xenopus* embryos, TGFβRII can replace ACTRIIB for binding to Activin and/or TGFβ and induce mesoderm formation (41).

From a functional perspective, Nodal's critical role in self renewal and maintenance of the stem cell-like characteristics of metastatic melanoma cells is well established (6). In addition, Nodal plays a quintessential role in tumor cell vasculogenic mimcry (VM)—the *de novo* formation of perfusable networks by aggressive tumor cells in 3D matrices *in vitro*, which mimics matrix-rich networks found in patient's tumors, and reflects a plastic, functional endothelial phenotype expressed by aggressive melanoma cells (42). Nodal associates with networks in human melanoma xenografts (43), and down-regulation of Nodal inhibits the network formation by metastatic melanoma cells (44). However, receptor usage relevant to Nodal signaling and temporal/spatial positioning of Nodal associated with these structures remain mostly unexplored. Interestingly, the expression of the endothelial-specific marker VE-cadherin is also a feature of metastatic melanoma cells and a marker of their plasticity, especially pertinent to VM (45). Our studies indicate C8161 cells form ECM-rich structures of “loops and nests” on plastic substrate and organized VM tubular networks on Matrigel, while the DNC8161 counterpart fails to do so and remains as a monolayer on plastic substrate, and forms cellular clumps on Matrigel (Fig.4). Immunofluorescence confocal microscopy indicated an intracellular association of Nodal and membrane association of VE-cadherin in C8161 cells grown on glass substrate (Fig. 5Aa). At early stages of VM assembly on Matrigel, Nodal was mostly concentrated at the outer edge of the VM networks, often in association with either VE-cadherin or TGFβRII (Fig. 5A b & d). DNC8161 cells grown on glass substrate exhibit disrupted membrane-associated VE-cadherin (translocating into the cytoplasm and nucleus; Fig. 5Ae), and no organized structures on Matrigel (Fig.5A, f & h). Addition of rNodal to DNC8161 cultures did not restore VM (Sup. Fig.2). However, some of these aggregates ultimately spread and form unorganized structures over time (data not shown).

Treatment of C8161 melanoma cells with antibody to Nodal (which reduces the intracellular Nodal protein levels through a negative feedback loop) down-regulates TGFβRII (Fig.3 A), abolishes C8161 cell's ability to form “loops and nests” on plastic substrate and impedes the proper formation of organized VM networks on Matrigel, ultimately leading to substantial cell death (Sup. Fig.3). Clearly, Nodal's presence at the outer edges of the VM networks, and its association with TGFβRII (Fig. 5A b & d) is important in proper assembly and maintenance of these structures. Of special interest, non-aggressive melanoma cell lines express much lower levels of TGFβ-RII, and do not form the VM structures on plastic substrate or organized tubular networks on Matrigel (Sup. Fig.4). However, overexpression of TGFβ-RII in non-aggressive melanoma cell lines fails to promote VM tubular network formation. These cell lines express little to no Nodal (compared to aggressive melanoma lines), and it is likely that Nodal-TGFβ-RII interaction requires a certain threshold of cellular Nodal, as rNodal treatment of the TGFβ-RII-transfected non-aggressive melanoma cells exerts no effect on VM formation (Sup. Fig.4). Also noteworthy is the participation of other pathways (i.e. NOTCH, VEGF) and their required coordinated expression in melanoma cell-

mediated formation of VM networks (42). The subtle nuances in C8161 responses to blocking Nodal and TGFβRII likely reflect their involvement in other cellular functions.

Long term cultures of metastatic melanoma cells on Collagen I matrices generated more developed (hollow looking) tubular structures (previously shown in Fig. 4E; solid arrows) lined with flattened endothelial-like melanoma cells (Fig.5B, yellow arrows and Sup.Fig. 5). Nodal was predominantly at the peri-tubular surface of these structures, while VE-cadherin exhibited a luminal position. The formation of these hollow vascular tubular structures is reminiscent of that reported in aggressive ovarian cancers, as demonstrated by transmission electron microscopy (46). It is important to note that neutralizing Pan-TGFβ antibody, despite its modest effect on Smad2/3 phosphorylation, failed to inhibit VM network formation by metastatic melanoma cells (Sup. Fig. 6), further supporting the specificity of the Nodal signaling pathway.

In conclusion, we report for the first time the receptor usage for propagating Nodal signaling underlying plasticity in aggressive melanoma compared with hESCs. In hESCs, the heterodimeric ACTRII/ACTRI complex is recruited for Nodal signaling, while in metastatic melanoma cells, low abundance of ACTRII dictates an alternate use of the TGFβR II/ TGFβR I complex to achieve comparable effects, as summarized in Figure 6. This signaling pathway is critical for VM commonly associated with the plastic, aggressive melanoma phenotype (42), and also found in carcinoma, sarcoma, glioma, glioblastoma and astrocytoma (reviewed in 47,48). The majority of these cancer types express Nodal and TGFβRII/TGFβRI (highlighted in Supplemental Table 1); however, whether Nodal utilizes these receptors universally across all cancers remains to be determined—important information that could impact new therapeutic strategies.

Supplementary Material

Refer to Web version on PubMed Central for supplementary material.

ACKNOWLEDGEMENT

This work was supported by NIH/RO1 CA121205, R37 CA59702 and U54 CA143869 (to MJCH). The authors gratefully acknowledge Dr. Harold Moses, Dept. of Cancer Biology and Medicine, Vanderbilt-Ingram Cancer Center, Nashville, Tennessee for the generous gift of dominant negative TGFβRII plasmid.

REFERENCES

1. Schier AF. Nodal signaling in vertebrate development. Annu Rev Cell Dev Biol. 2003; 19:589–621. [PubMed: 14570583]
2. Shen MM. Nodal signaling: developmental roles and regulations. Development. 2007; 134:1023–1034. [PubMed: 17287255]
3. James D, Levine AJ, Besser D, Hemmati-Brivanlou A. TGFbeta/activin/nodal signaling is necessary for the maintenance of pluripotency in human embryonic stem cells. Development. 2005; 132:1273–1282. [PubMed: 15703277]
4. Vallier L, Alexander M, Pedersen R A. Activin/Nodal and FGF pathways cooperate to maintain pluripotency of human embryonic stem cells. J Cell Sci. 2005; 118:4495–4509. [PubMed: 16179608]
5. Branford WW, Yost HJ. Lefty dependent inhibition of Nodal- and Wnt-responsive organizer gene expression is essential for normal gastrulation. Curr Biol. 2002; 2:2136–2141. [PubMed: 12498689]

6. Topczewska JM, Postovit L-M, Margaryan NV, Sam A, Hess AR, Wheaton WW, Nickolaff BJ, Hendrix MJC. Embryonic and tumorigenic pathways converge via Nodal signaling: role in melanoma aggressiveness. Nat. Med. 2006; 12:925–932. [PubMed: 16892036]
7. Papageorgiou I, Nicholls PK, Wang F, Lackmann M, Makanji Y, Salamonsen LA, Robertson DM, Harrison CA. Expression of nodal signalling components in cycling human endometrium and in endometrial cancer. Rep Biol and Endocrinol. 2009; 7:122–132.
8. Lee C-C, Jan H-J, Lai J-H, Ma H-I, Hueng D-Y, Gladys Lee Y-C, Cheng Y-Y, Liu L-W, Wei HW, Lee H-M. Nodal promotes growth and invasion in human gliomas. Oncogene. 2010; 29:3110–3123. [PubMed: 20383200]
9. Lawrence MG, Margaryan NV, Loessner D, Collins A, Kerr KM, Turner M, Seftor EA, Stephens CR, Lai J, Postovit LM, Clements JA, Hendrix MJC. Reactivation of embryonic Nodal signaling is associated with tumor progression and promotes the growth of prostate cancer cells. Prostate. 2011; 71:1198–1209. [PubMed: 21656830]
10. Lonardo E, Hermann PC, Mueller M-T, Huber S, Balic A, Miranda-Lorenzo I, Zagorac S, Alcala S, Rodriguez-Arabaolaza I, Ramirez JC, Torres-Ruíz I, Garcia E, et al. Nodal/Activin signaling drives self-renewal and tumorigenicity of pancreatic cancer stem cells and provides a target for combined drug therapy. Cell Stem Cell. 2011; 9:433–446. [PubMed: 22056140]
11. Strizzi L, Hardy KM, Margaryan NV, Hillman DW, Seftor EA, Chen B, Geiger XJ, Thompson EA, Lingle WL, Andorfer CA, Perez EA, Hendrix MJC. Potential for the embryonic morphogen Nodal as a prognostic and predictive biomarker in breast cancer. Breast Cancer Res. 2012; 1:R754.
12. Costa FF, Seftor EA, Bischof JM, Kirschmann DA, Strizzi L, Arndt K, Bonaldo MF, Soares MB, Hendrix MJC. Epigenetically reprogramming metastatic tumor cells with an embryonic microenvironment. Epigenomics. 2009; 1:387–398. [PubMed: 20495621]
13. Sakuma R, Ohnishi Yu-I, Meno C, Fujii H, Juan H, Takeuchi J, Ogura T, Li E, Miyazono K, Hamada H. Inhibition of Nodal signaling by Lefty mediated through interaction with common receptors and efficient diffusion. Genes Cell. 2002; 7:401–412.
14. Ben-Haim N, Guzma-Ayala M, Pescatore L, Mesnard D, Bischofberger M, Naef F, Robertson EJ, Constam DB. The Nodal precursor acting via activin receptors induces mesoderm by maintaining a source of its convertases and BMP-4. Dev. Cell. 2006; 11:313–323. [PubMed: 16950123]
15. Gary PC, Harrison CA, Vale V. Cripto forms a complex with activin and type II activin receptors and can block activin signaling . Proc Nat Acad Sci USA. 2003; 100:5193–5198. [PubMed: 12682303]
16. Yan YT, Liu JJ, Luo Y, E C, Haltiwanger RS, Abate-Shen C, Shen MM. Dual role of Cripto as a ligand and coreceptor in the Nodal signaling pathway. Mol Cell Biol. 2002; 22:1–11. [PubMed: 11739717]
17. Watanabe K, Salomon DS. Intercellular transfer of the paracrine activity of GPI-anchored Cripto-1 as a Nodal co-receptor. Biochem Biophys Res Commun. 2010; 403:108–113. [PubMed: 21055389]
18. Welch DR, Bisi JE, Miller BE, Conaway D, Seftor EA, Yohem KH, Gilmore LB, Seftor RE, Nakajima M, Hendrix MJ. Characterization of a highly invasive and spontaneously metastatic human malignant melanoma cell line. Int. J. Cancer. 1991; 47:227–237. [PubMed: 1671030]
19. van Muijen GN, Jansen KF, Cornelissen IM, Smeets DF, Beck JL, Ruiter DJ. Establishment and characterization of a human melanoma cell line (MV3) which is highly metastatic in nude mice. Int. J. Cancer. 1991; 48:85–91. [PubMed: 2019461]
20. Bittner M, Meltzer P, Chen Y, Jiang Y, Seftor E, Hendrix M, Radmacher M, Simon R, Yakhini Z, Ben-Dor A, Sampas N, Dougherty E, et al. Molecular classification of cutaneous malignant melanoma by gene expression: Shifting from a continuous spectrum to distinct biologic entities. Nature. 2000; 406:536–540. [PubMed: 10952317]
21. Thomson SP, Meyskens FL Jr. Method for measurement of self-renewal capacity of clonogenic cells from biopsies of metastatic human malignant melanoma. Cancer Res. 1982; 42:4606–13. [PubMed: 7127298]
22. Khalkhali-Ellis Z, Abbott DE, Bailey CM, Goossens W, Margaryan NV, Gluck SL, Reuveni M, Hendrix MJC. IFN-gamma regulation of vacuolar pH, cathepsin D processing and autophagy in mammary epithelial cells. J Cell Biochem. 2008; 105:208–218. [PubMed: 18494001]

23. Zúñiga JE, Groppe JC, Cui Y, Hinck CS, Contreras-Shannon V, Pakhomova ON, Yang J, Tang Y, Mendoza V, López-Casillas F, Sun L, Hinck AP. Assembly of TGFβRI: TGFβR II: TGFβ ternary complex in vitro with receptor extracellular domains is cooperative and isoform-dependent. J Mol Biol. 2005; 354:1052–1068. [PubMed: 16289576]
24. Kim YW, Park J, Lee HJ, LEE SY, Kim S-J. TGFβ sensitivity is determined by N-linked glycosylation of the type II receptor. Biochem J. 2012; 445:403–411. [PubMed: 22571197]
25. Strizzi L, Postovit L-M, Margaryan NV, Lipavsky A, Gadiot J, Blank C, Seftor REB, Seftor EA, Hendrix MJC. Nodal as biomarker for melanoma progression and a new therapeutic target for clinical intervention. Expert Rev Dermatol. 2009; 4:67–78. [PubMed: 19885369]
26. Reissmann E, Jornvall H, Blokzijl A, Anderson O, Chang C, Minchiotti G, Persico MG, Ibanez CF. The orphan receptor ALK 7 and Activin receptor ALK4 mediate signalling by Nodal proteins during vertebrate development. Genes Dev. 2001; 15:2010–2022. [PubMed: 11485994]
27. Yeo C, Withman M. Nodal signals to Smads through Cripto-dependent and Cripto-independent mechanisms. Mol Cell. 2001; 7:949–9957. [PubMed: 11389842]
28. Massaque J, Seoane J, Wotton D. Smad transcription factors. Gene Dev. 2005; 19:2783–27810. [PubMed: 16322555]
29. Groppe J, Hinck CS, Samavarchi-Tehrani P, Zubieta C, Schuermann JP, Taylor AB, Schwarz PM, Wrana JL, Hinck AP. Cooperative assembly of TGFβ superfamily signaling complex is mediated by two disparate mechanisms and distinct modes of receptor binding. Mol Cell. 2008; 29:157–168. [PubMed: 18243111]
30. Baardsnes J, Hinck CS, Hinck AP, Occoner–McCourt. TGFβRII discriminate the high-and low-affinity TGFβ isoforms via two hydrogen-bounded ion pairs. Biochemistry. 2009; 48:2146–2155. [PubMed: 19161338]
31. Radaev S, Zou Z, Huang T, Lafer EM, Hinck AP, Sun PD. Ternary complex of of TGFβ-1 reveals isoform-specific ligand recognition and receptor recruitment in the superfamily. J Biol Chem. 2010; 285:14806–14814. [PubMed: 20207738]
32. López-Casillas F, Wrana JL, Massagué J. Betaglycan presents ligand to the TGF beta signaling receptor. Cell. 1993; 73:1435–1444. [PubMed: 8391934]
33. López-Casillas F, Payne HM, Andres JL, Massagué J. Betaglycan can act as a dual modulator of TGF-beta access to signaling receptors: mapping of ligand binding and GAG attachment sites. J Cell Biol. 1994; 124:557–568. [PubMed: 8106553]
34. Laping NJ, Grygielko E, Mathur A, Butter S, Bomberger J, Tweed C, Martin W, Fornwald J, Lehr R, Harling J, Gaster L, Callahan JF, et al. Inhibition of TGFβ-1-induced extracellular matrix with a novel inhibitor of TGFβ type I receptor kinase activity:SB431542. Mol Pharmacol. 2002; 62:58–64. [PubMed: 12065755]
35. Chen RH, Ebner R, Derynck R. Inactivation of type II receptor reveals two receptor pathways for the diverse TGFβ activities. Science. 1993; 260:1335–1338. [PubMed: 8388126]
36. Derynck R, Feng X-H. Smad-dependent and Smad-independent pathways in TGF-β family signaling. Nature. 2003; 425:577–584. [PubMed: 14534577]
37. Itoh S, Itoh F, Goumans MJ, ten Dijke P. Signaling of transforming growth factor –beta family members through Smad proteins. Eur J Biochem. 2000; 267:6954–6967. [PubMed: 11106403]
38. Sebald W, Nickel J, Zhang JL, Mueller TD. Molecular recognition in bone morphogenic protein (BMP)/receptor recognition. Biol Chem. 2004; 385:697–710. [PubMed: 15449706]
39. Upton PD, Davis RJ, Trembath RC, Morrel NW. Bone morphogenic protein and Activin type II receptors balance BMP9 signals mediated by Activin receptor-like kinase-1in human pulmonary artery endothelial cells. J Biol Chem. 2009; 284:15794–15804. [PubMed: 19366699]
40. Liu H, Zhang R, Chen D, Oyajobi BO, Zhao M. Functional redundancy of type II BMP receptor and type IIB Activin receptor in BMP-induced osteoblast differentiation. J Cell Physiol. 2012; 227:952–963. [PubMed: 21503889]
41. Bhushan A, Lin HY, Lodish HF, Kintner CR. The TGR-βRII can replace the Activin type II receptor in inducing mesoderm. Mol Cell Biol. 1994; 14:4280–4285. [PubMed: 8196664]
42. Kirschmann DA, Seftor EA, Hardy KM, Seftor REB, Hendrix MJC. Molecular pathways: Vasculogenic mimicry in tumor cells:diagnostic and therapeutic implications. Clin Cancer Res. 2012; 18:1–7.

43. McAlister JC, Zhan Q, Weisthaupt C, Hsu M-Y, Murphy G. The embryonic morphogen Nodal is associated with channel-like structures in human malignant xenografts. J Cutaneous Pathol. 2010; 37:19–25.

44. Strizzi L, Hardy KM, Seftor EA, Margaryan NV, Kirschmann DA, Kirsammer GT, Bailey CM, Kasemeire-Kulesa JC, Kulesa PM, Seftor EB, Hendrix MJC. Lessons from embrygenesis. Melanoma Dev. 2011; 13:281–296.

45. Hendrix MJC, Seftor EA, Meltzer PS, Gardner LM, Hess AR, Kirschmann DA, Schatterman GC, Setor REB. Expression and functional significance of VE-cadherin in aggressive human melanoma cells. Role in vasculogenic mimicry. Proc Nat Acad Sci USA. 2001; 98:8018–8023. [PubMed: 11416160]

46. Sood A, Seftor EA, Fletcher MS, Gardner LMG, Heidger PM, Buller RE, Seftor REB, Hendrix MJC. Molecular determinants of ovarian cancer plasticity. Amer J Pathol. 2001; 158:1279–1288. [PubMed: 11290546]

47. Hendrix MJC, Seftor EA, Hess AR, Seftor REB. Vasculogenic mimicry and tumor cell plasticity: lessons from melanoma. Nat Rev Cancer. 2003; 3:411–421. [PubMed: 12778131]

48. Paulis YWJ, Soetekouw PM, Verhheul HMW, Tjan-Heijnen VCG, Griffioen AW. Signalling pathways in vasculogenic mimicry. Biochem Biophys Acta. 2010; 1806:18–28. [PubMed: 20079807]

Novelty and Impact

Our studies delineate a previously unidentified receptor usage for Nodal in metastatic melanoma and define its function in maintaining the plasticity of melanoma tumor cells. These findings will assist in developing tailored therapeutic approaches to target cancers which share similar mechanism(s) for propagating Nodal's signal.

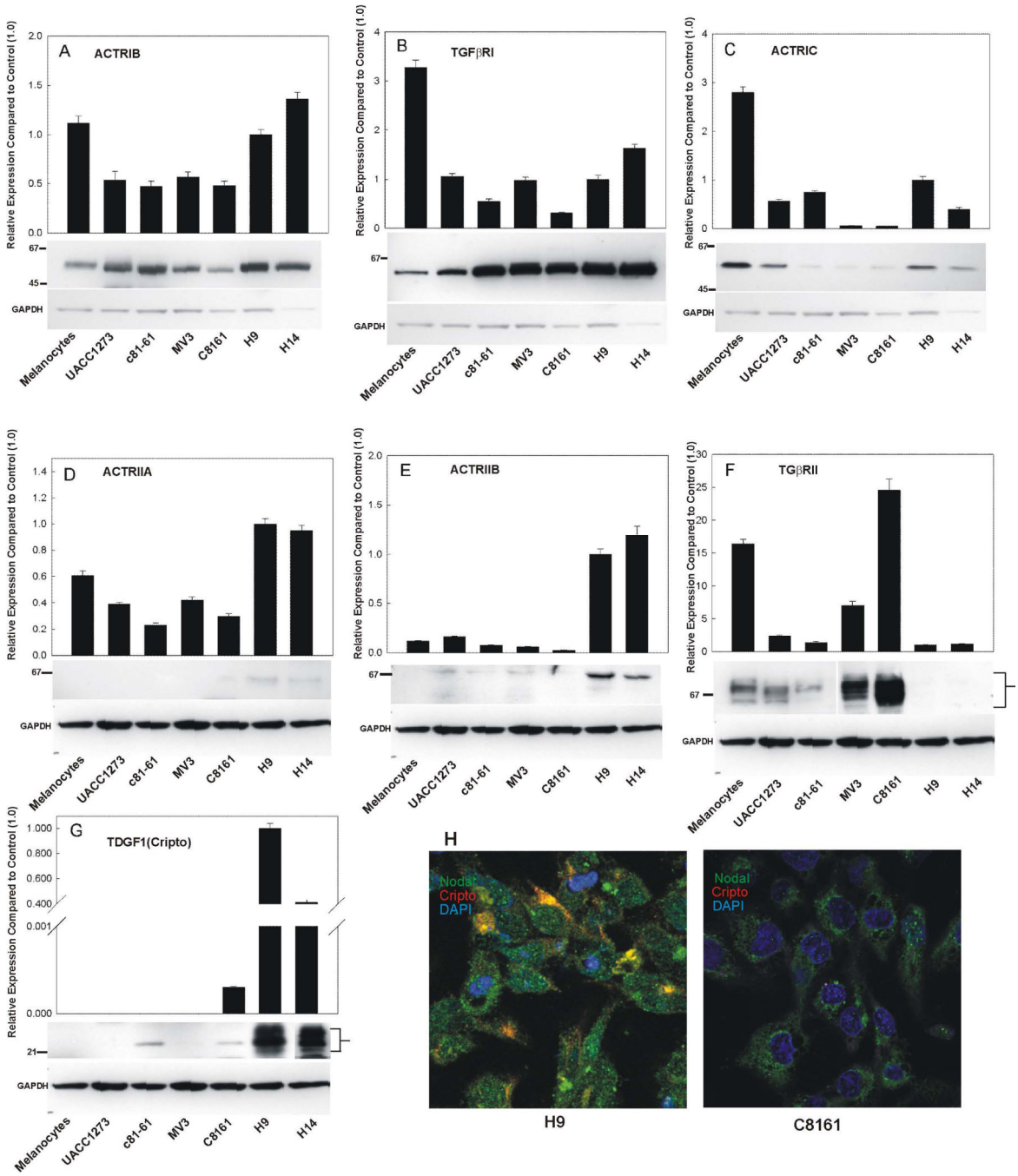

Fig.1.

Receptor profiling performed at the mRNA and protein levels of hESCs and human melanoma cell lines (with human melanocytes serving as a control). Histograms depict real time RT-PCR analysis of the TGFβ/Nodal receptors in human cell lines representative of metastatic melanoma (C8161, MV3), non-aggressive melanoma (UACC1273, c81-61), and melanocytes vs. H9 and H14 hESCs, where data are normalized to RPLPO and relative expression compared to that of H9 (set at 1.0). The Western blot analyses of the protein products of each gene (along with the GAPDH loading control) are provided underneath the

respective histogram. For consistency and when possible, each Western blot was re-probed several times; ACTRIB, ACTRIC, and TGFβRI were probed consecutively on the same blot and share a common GAPDH loading control. Similarly, ACTRIIA, ACTRIIB, TGFβRII and Cripto were probed from the same blot and share a common GAPDH loading control. Different glycosylated (or phosphorylated) forms of the receptors are marked on the right hand side of the specific blots. Due to the lower abundance of TGFβRII in the non-metastatic melanoma cells, a longer exposure is presented for clear depiction of different forms of receptor. (H) Immunofluorescence confocal imaging of H9 hESC vs. C8161 melanoma cells demonstrates divergent expression of Cripto (TDGF1). Confocal imaging was performed on a Zeiss LSM-510 META confocal laser scanning microscope equipped with ZEN software. Nodal: 488 (green), Cripto; 660 (red), nucleus: DAPI (blue). In H9 hESCs, Cripto appears often co-localized with Nodal (generating a yellow fluorescence). Barely detectable Cripto is shown in C8161 cells. Original magnification: 63×.

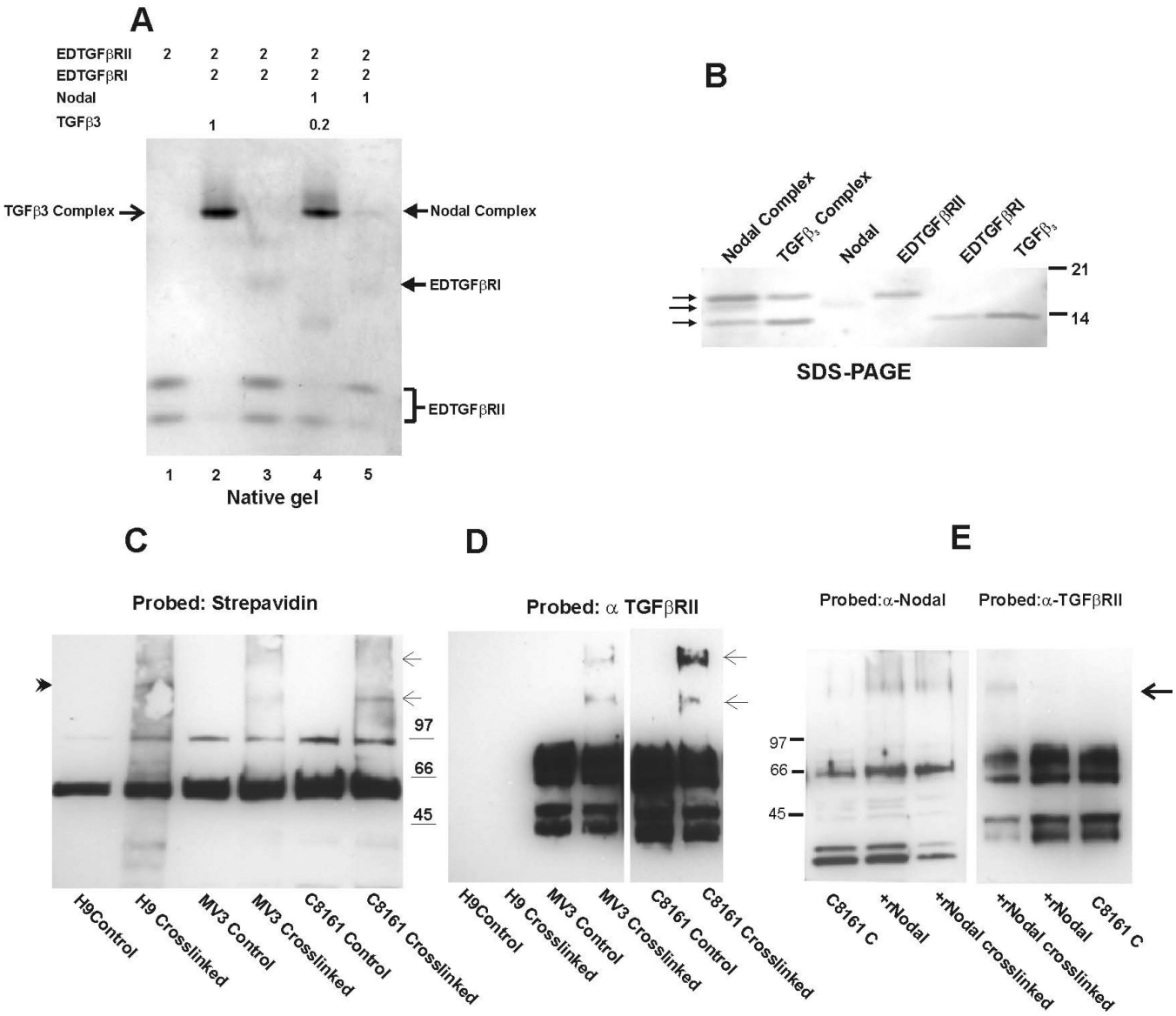

Fig.2.

In vitro binding assay and ligand-receptor crosslinking implemented to identify Nodal receptor usage. (A) Qualitative native gel binding assay indicates complex formation between Nodal, EDTGFβRII and EDTGFβRI. The recombinant proteins were mixed in the molar ratios noted (37° C, 30min), and the mixture was applied to a 12.5% native acrylamide gel, followed by Commassie staining of the gel. Compared to the complex formed by TGFβ3 (lane 2), Nodal weakly binds the receptors, and TGFβ3 competes with Nodal in receptor binding (lane 4). The position of EDTGFβRI and EDTGFβRII are indicated in the figure; EDTGFβRII runs as two discreet bands, caused by the strong propensity of Asparagine 19 to deamidate and form Aspartic acid, which gives the protein an additional charge. (B) The bands corresponding to the complexes formed were excised, taken up in sample buffer and analyzed by SDS-PAGE (4-20% acrylamide) and Western blot for the presence of EDTGFβRII, Nodal, and EDTGFβRI (indicated by arrows in

descending order). (C) Biotin-labeled ligand crosslinking of cell surface receptors reveals products with different molecular mass in metastatic melanoma cells (C8161 and MV3) compared to H9 hESCs. Following the crosslinking of the cell surface receptors with Biotin-labeled-Nodal, membrane fractions were prepared and subjected to SDS-PAGE and Western blot analysis with Strepavidin. Strepavidin reactive bands are indicated by arrows (C8161 and MV3), and arrowhead (H9). (D) The blot was stripped and reprobed with antibody to TGFβRII, the arrows also denote the Strepavidin reactive bands cross-reacting with anti-TGFβRII. As MV3 cells have a lower level of TGFβRII, a longer exposure of that section of the blot is included in this figure. (E) Nodal was detected in the complex formed in C8161 cells, but was barely detectable in MV3 complex (data not shown). Arrow indicates the additional anti-TGFβRII reactive band following crosslinking.

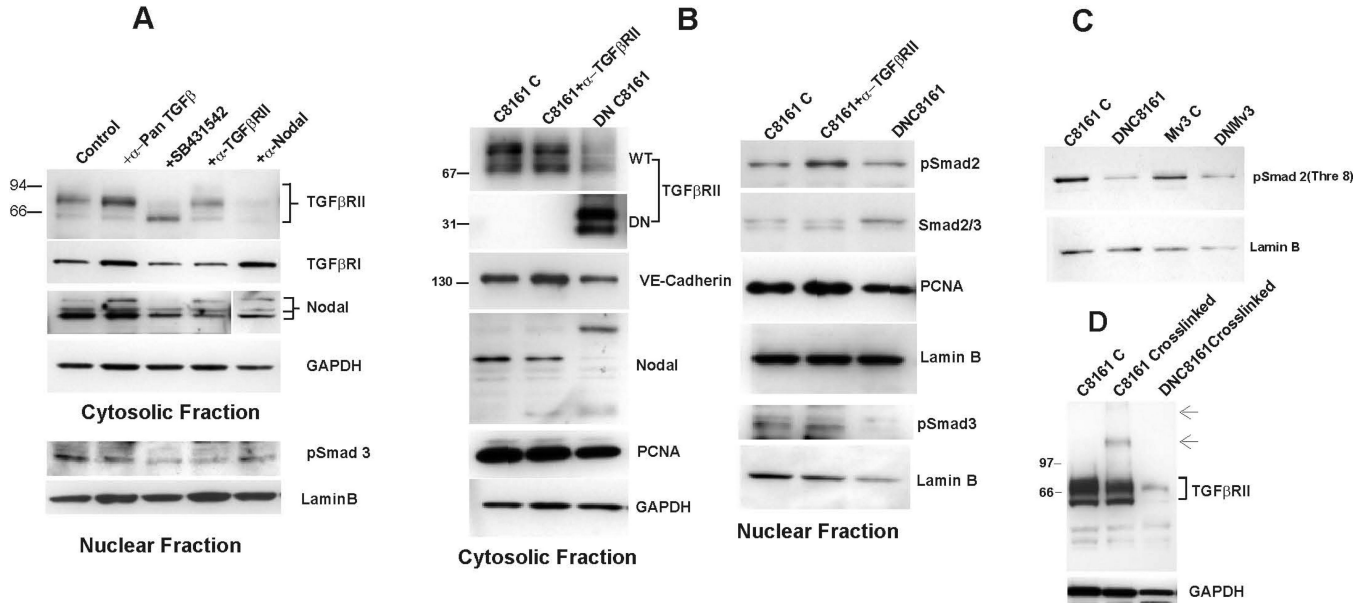

Fig.3.

Functional inhibition of TGFβRII with neutralizing antibody or transfection of cells with DNTGFβRII affected Nodal expression and downstream Smad2/3 phosphorylation in metastatic melanoma cells. These effects were comparable to those observed with the small molecule kinase inhibitor SB431542 (A,B). DNTGFβRII also reduced the cellular proliferation (indicated by changes in cytosolic and nuclear PCNA levels), and often changed Nodal processing (B). Nodal antibody treatment (3μg/ml, 72hr), which reduced the intracellular Nodal protein levels, attenuated TGFβRII protein levels considerably (compare lanes 4 and 5 in Fig.3A). Pan-TGFβ antibody reduced Smad3 phosphorylation, but had minimal effect on Nodal expression (A). (C) In addition to Serine phosphorylation of Smad2/3, DNTGFβRII transfection reduced the constitutively phosphorylated Threonine 8 in Smad2. (D) In the crosslinking approach, DNTGFβRII competed with the wild type TGFβRII for binding the ligand in aggressive melanoma cell lines employed. The arrows indicate additional anti- TGFβRII reactive bands.

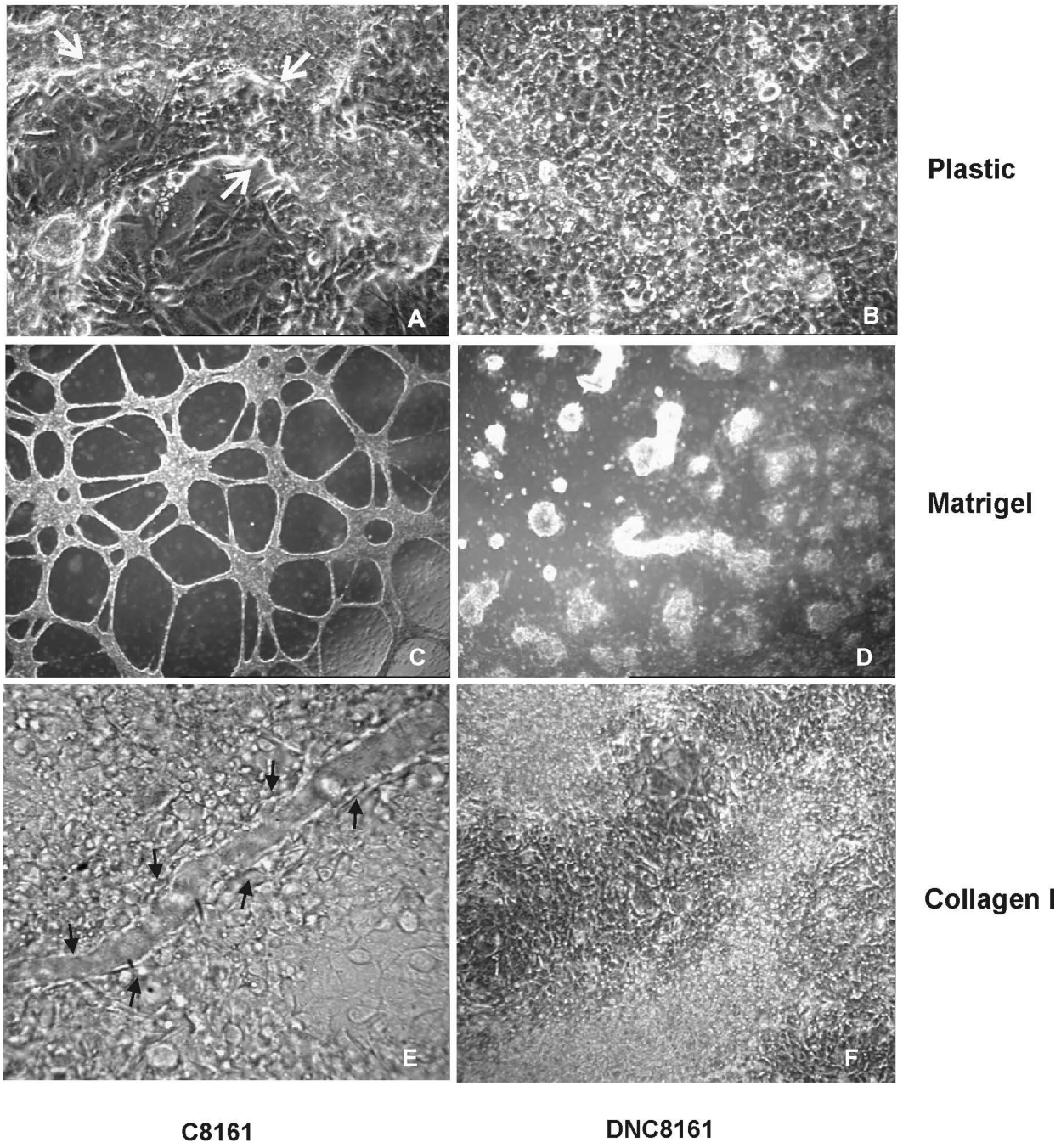

Fig.4.

Phase contrast microscopy of C8161 and DNC8161 melanoma cells exhibit distinct cellular morphology on different matrices. C8161 cells grown on plastic substrate generate VM networks (4A, arrows), while DN C8161 cells fail to do so and remain as a monolayer (4B). Likewise, when plated on Matrigel, C8161 cells formed ECM-rich capillary-like network structures (4C), while their DN C8161 counterpart grows in clumps and forms aggregates (4D). Long term cultures of C8161 on 3D Collagen I resulted in the formation of more

developed tubular structures (4E, arrows), while DN C8161 cells fail to form any structures (4F). Original magnification, 10×.

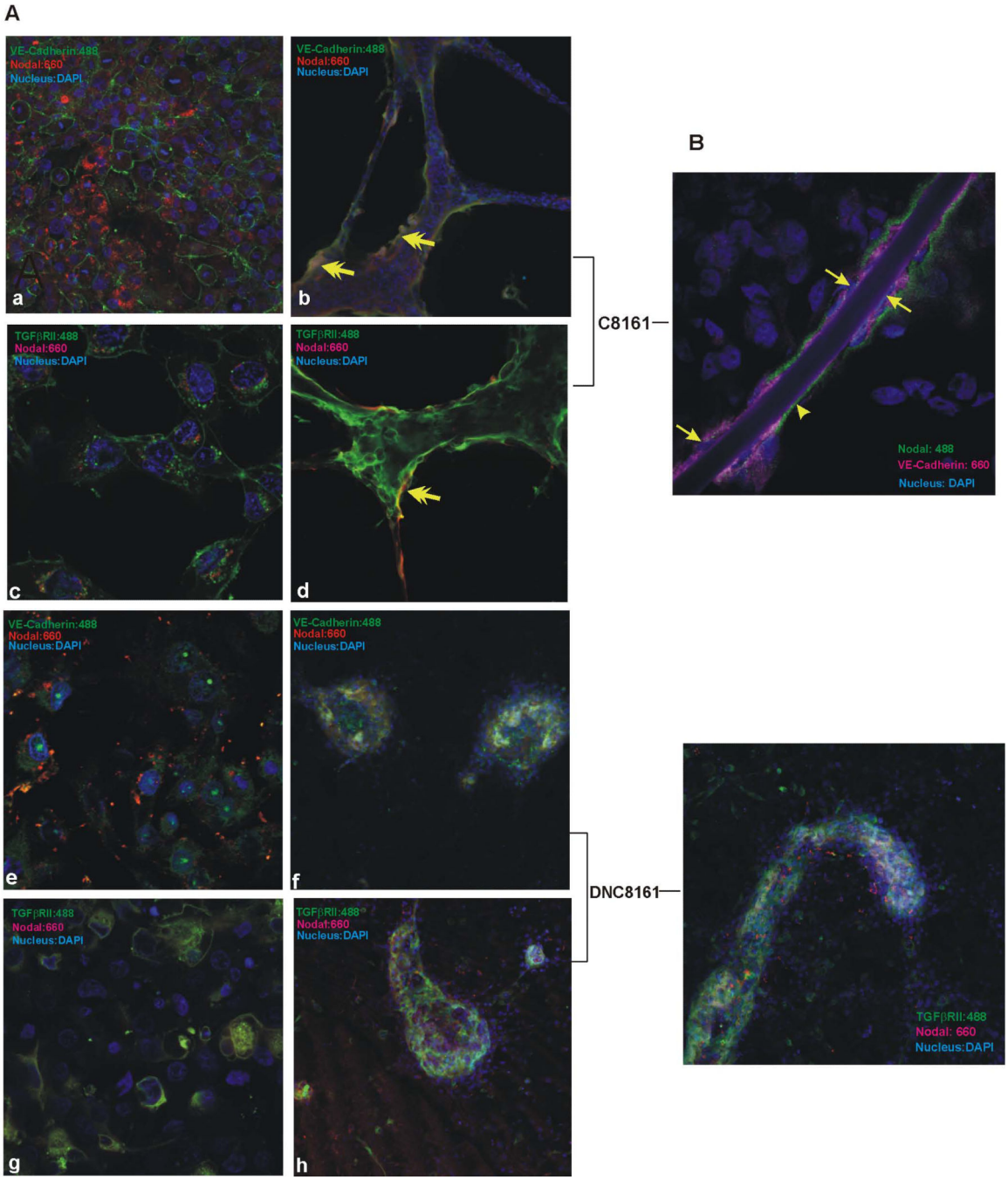

Fig.5.

Confocal immunofluorescence analyses of C8161 and DNC8161 cells grown on different matrices and for variable culture periods demonstrate distinct spatial distribution of Nodal. (A) Both C8161 (a, c), and DNC8161 cells (e, g) grown on glass substrate display an intracellular distribution of Nodal. On Matrigel, C8161 cells form vascular-like networks with Nodal mostly detected at the outer edge of the network structures, often in association with VE-cadherin or TGFβRII (yellow arrows, b & d). DN C8161 only forms unstructured clumps on Matrigel with no specific distribution of Nodal (f &h). (B) Long term cultures

(16-20 days) of C8161 on 3D Collagen I matrices resulted in the formation of more developed hollow-appearing tubular structures (as shown previously in Fig. 4e by phase contrast microscopy). Elongated tumor cells (yellow arrows) delineate the tubular structures. These endothelial-like melanoma cells appear polarized based on their peri-tubular expression of Nodal and luminal expression of VE-cadherin. DNC8161 placed on Collagen I initially formed clumps; however, the clumps slowly spread and at the end of 2.5 weeks in culture, minor structures could be observed without the alignment of the tumor cells (for quadrant display of the colors in (B), see Sup. Fig. 5). Nuclei are stained with DAPI (blue). Original magnification, 63X.

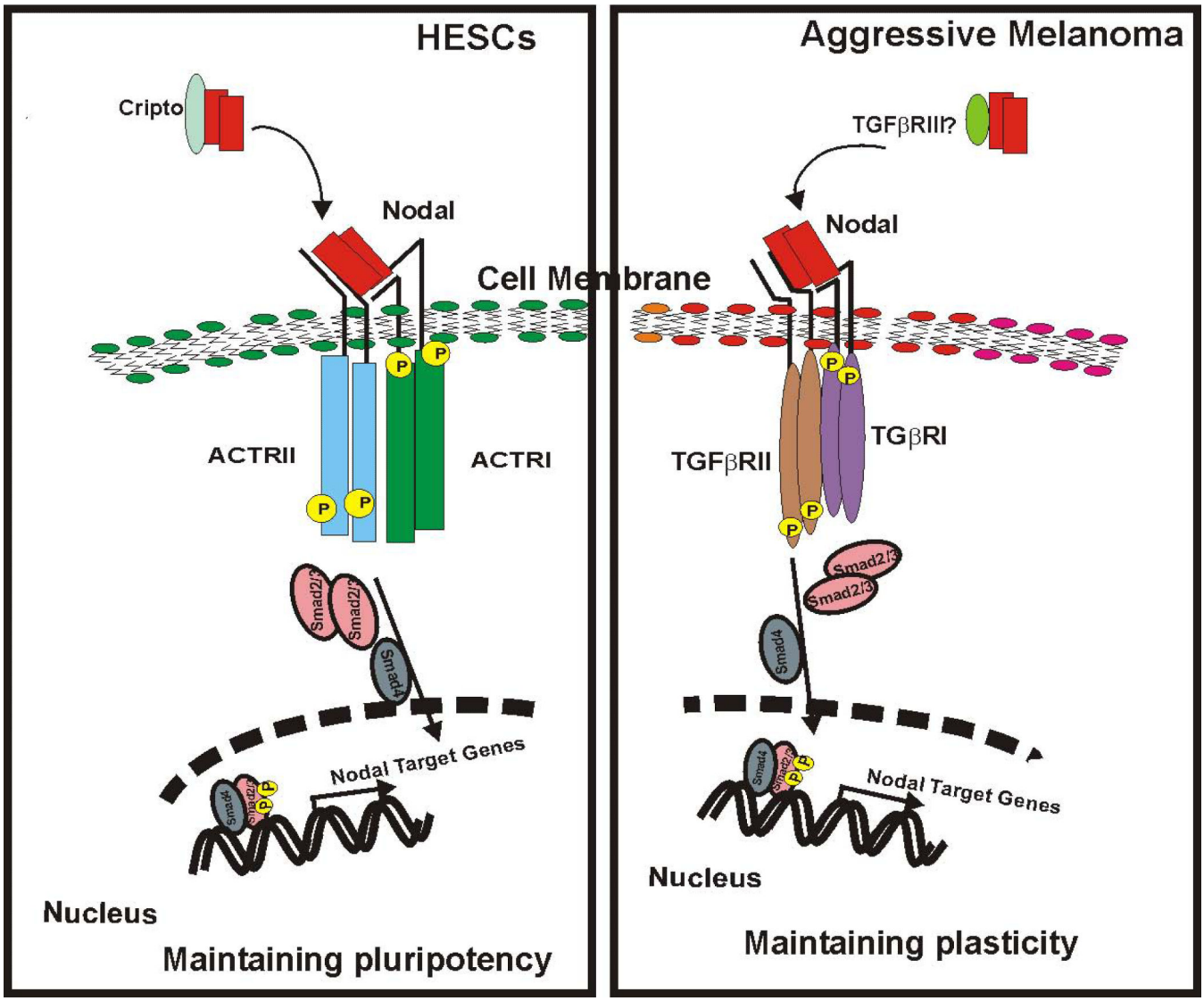

Fig.6.

Schematic overview of differential signaling machinery employed by Nodal in hESCs compared to aggressive melanoma cells.